frontiers | Frontiers in Earth Science

TYPE Original Research
PUBLISHED 26 September 2022
DOI 10.3389/feart.2022.967043

OPEN ACCESS

EDITED BY
Karoly Nemeth,
Massey University, New Zealand

REVIEWED BY
Jorge Eduardo Romero,
Universidad de Atacama, Chile
Anke Verena Zernack,
Massey University, New Zealand

*CORRESPONDENCE
Mitsuhiro Nakagawa,
mnakagawa@sci.hokudai.ac.jp

SPECIALTY SECTION
This article was submitted to Volcanology,
a section of the journal
Frontiers in Earth Science

RECEIVED 12 June 2022
ACCEPTED 19 August 2022
PUBLISHED 26 September 2022

CITATION
Nakagawa M, Matsumoto A and Yoshizawa M (2022), Re-investigation of the sector collapse timing of Usu volcano, Japan, inferred from reworked ash deposits caused by debris avalanche.
Front. Earth Sci. 10:967043.
doi: 10.3389/feart.2022.967043

Re-investigation of the sector collapse timing of Usu volcano, Japan, inferred from reworked ash deposits caused by debris avalanche

Mitsuhiro Nakagawa*, Akiko Matsumoto and Mitsuki Yoshizawa

Department Natural History Sciences, Graduate School of Science, Hokkaido University, Sapporo, Japan

It is essential to establish the timing of past sector collapse events at a volcanic edifice to evaluate not only the evolution of the volcanic system but also potential volcanic hazards. This can be done by determining the age of the collapse-generated debris avalanche deposits. However, without evidence of an associated magmatic eruption, it is impossible to recognize juvenile materials in these deposits. Thus, it is usually difficult to determine the precise age of sector collapse. Usu is a post-caldera volcano of the Toya Caldera (Hokkaido, Japan) and has been constructed since ca. 19–18 ka on top of the caldera-forming Toya pyroclastic flow deposits (Tpfl deposit: 106 ka). A sector collapse occurred after the formation of a stratovolcano edifice and produced the Zenkoji debris avalanche (ZDA) deposit with reported ages ranging from >20 to 6 ka. We investigated the tephrostratigraphy preserved in the soil above the ZDA deposit and in the surrounding area and recognized fine ash fall deposits at two locations, above and east of the ZDA deposit. The glass shards within these deposits were correlated with several tephra layers with the majority being derived from Tpfl deposits. Thus, these ash deposits should be considered reworked tephra. A considerable number of hummocks in the ZDA deposit were also composed of deformed and fragmented Tpfl deposits, which suggests that the ZDA bulldozed and partially incorporated the Tpfl deposit on the flank of the volcano. Deformation and fragmentation of the non-welded soft silicic Tpfl deposit during the transport and emplacement of the ZDA produced an accompanying ash cloud, which deposited the observed glassy, fine, ash fall units. Radiocarbon dating of soil samples directly below and above the reworked ash deposits allowed dating the sector collapse to ca. 8 ka. This age is much younger than previously proposed results. Based on our findings, the transport and emplacement mechanism of the sector collapse should be revised. Our study shows that reworked ash layers caused by the flow of a debris avalanche can be used as an indicator of the timing of a sector collapse of the volcano.

KEYWORDS

sector collapse, debris avalanche, reworked tephra, Toya pyroclastic flow, tephrostratigraphy, Usu volcano

1 Introduction

A flank or sector collapse of a volcano instantly changes the shape of the edifice and produces a horseshoe scar and debris avalanche (Siebert, 1984; Ui et al., 2000; Bernard et al., 2021). Although collapse is a low frequency phenomenon, the generation of a debris avalanche poses a serious hazard to populated areas around the volcano (Cortes et al., 2010; Marques et al., 2019). Moreover, edifice failure can change the magma plumbing system of a volcano and subsequent volcanic activity (Manconi et al., 2009; Boudon et al., 2013; Watt, 2019). Thus, it is important to identify sector collapse events within the long-term growth history of a volcano (Zernack and Procter, 2021). To better understand the volcanic system and allow for hazard assessment and potential disaster mitigation, it is important to clarify both the frequency-magnitude of sector collapse and its trigger, transport and emplacement mechanisms.

In this frame, it is essential to determine the age of the related debris avalanche deposit to elucidate the timing of collapse. However, without evidence of an associated magmatic eruption, it is impossible to recognize juvenile materials in these deposits. Thus, geochronological methods cannot be directly applied to the material comprised in debris avalanche deposits. Although previous studies have reported K-Ar or Ar-Ar ages of lavas from the remnant edifice, lava fragments within debris avalanche deposits and/or lavas erupted after a sector collapse (e.g., Ownby et al., 2007; Gaylord and Neall, 2012; Costa et al., 2014; Marques et al., 2019), these data would indicate the maximum and/or minimum age of the sector collapse. In case of a sector collapse younger than tens of thousands of years, several studies found wood and/or charcoal in a debris avalanche and considered that the radiocarbon ages of these materials indicated the timing of the collapse (Cortes et al., 2010; Goto et al., 2019). However, if there is no obvious evidence that the ages of these materials indicate the ages of a debris avalanche deposit, the ages would also be the maximum timing limit. On the other hand,

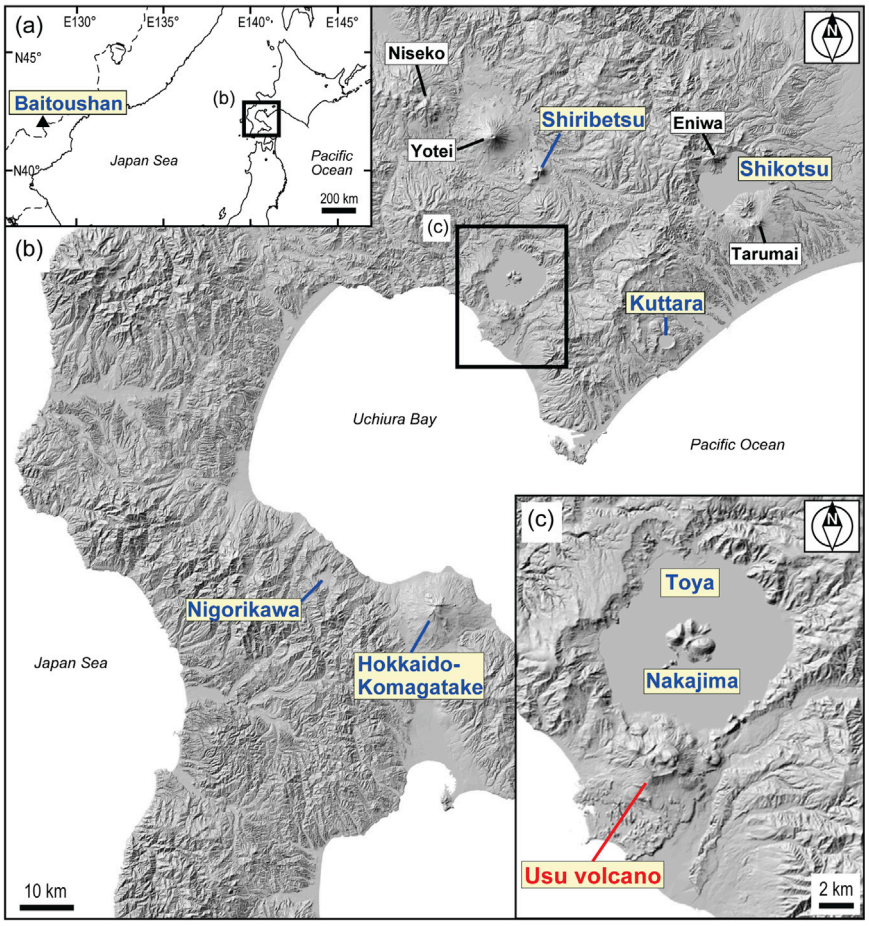

FIGURE 1
Overview map of Usu volcano and nearby volcanoes. Volcanoes in yellow-colored boxes are the source of tephras recognized around Usu volcano. Shaded-relief maps of **(B)** and **(C)** were created from digital topographic data provided by Geospatial Information Authority of Japan.

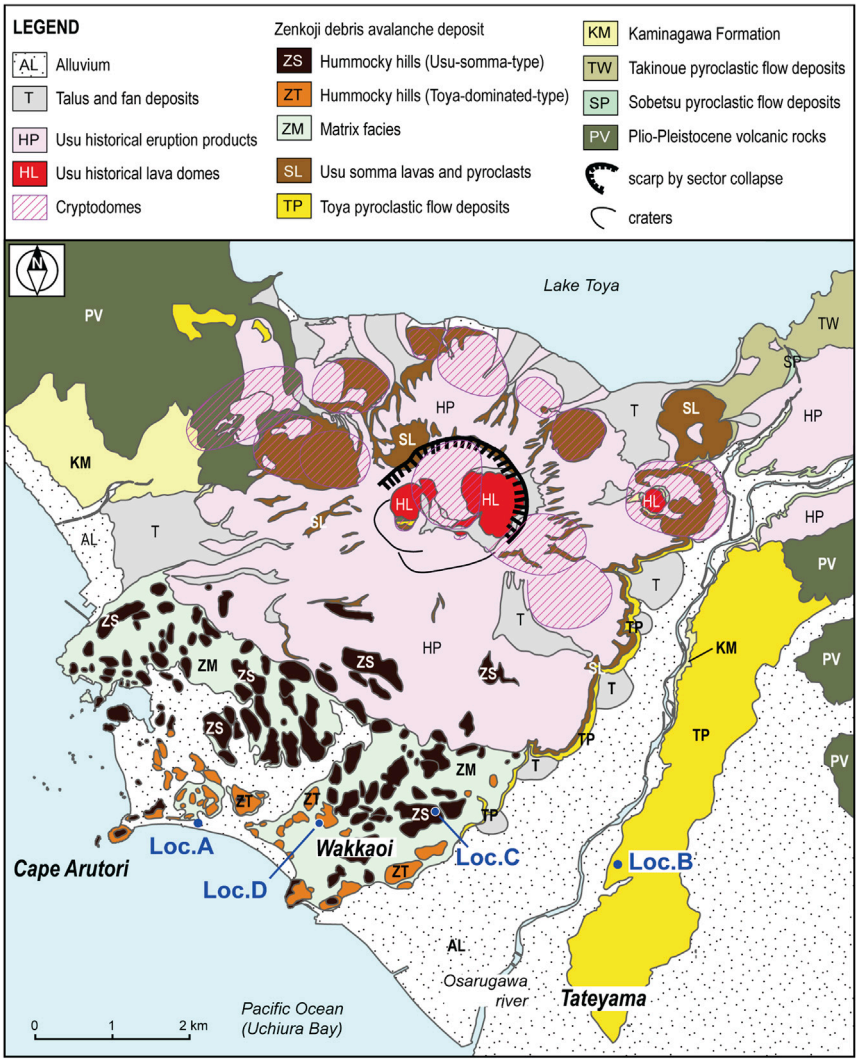

FIGURE 2
Geological map of Usu volcano, modified from Soya et al. (2007). Localities (A–D) on the map are the localities described in the text. Note that the distribution of the Kaminagawa Formation is limited to the west of Usu volcano and the base of the eastern cliff along the Osarugawa River.

several studies applied tephrochronology and radiocarbon dating to soil layers above and below a debris avalanche (Zernack et al., 2011; Fujine et al., 2016; Goto et al., 2019). However, a debris avalanche often erodes the ground surface during its flow (Ui et al., 2000; van Wyk de Vries et al., 2001; Yoshida and Sugai, 2007; Dufresne et al., 2021). Thus, the underlying soil does not necessarily represent the time immediately before a sector collapses. In summary, the ages of these deposits must be carefully investigated based on direct evidence that indicates the timing of collapse for each individual volcano.

Usu (Figure 1) is a post-caldera volcano of the Toya caldera, Japan (Yokoyama et al., 1973; Soya et al., 2007), and started its activity with a phreatomagmatic eruption at 19–18 ka (Goto et al., 2013). During the history of the volcano, a sector collapse of the edifice produced a debris avalanche deposit (the Zenkoji debris avalanche deposit, ZDA deposit). After the collapse, a long dormant period existed until historical activity began in AD 1663 (Yokoyama et al., 1973; Soya et al., 2007). Although the timing of the sector collapse has been investigated, the reported ages range from >20 to 6 ka (Oshima, 1968; Yokoyama et al., 1973; Kobayashi et al., 2006; Soya et al., 2007; Miyabuchi et al., 2014; Fujine et al., 2016; Goto et al., 2019). Since Usu is a young volcano with a history of ca. 20 kyr, the inconsistency in the reported ages has caused uncertainty in the evaluation of the volcanic processes at Usu volcano, such as magma

TABLE 1 List of marker tephra layers around Usu volcano.

Unit	Volcano	Age(ka)	References	Mineral assemblage
Us-b	Usu	AD1663	(1)	plg, opx, opq (±hbl, cpx)
Ko-d	Hokkaido-Komagatake	AD1640	(2)	plg, opx, cpx, opq
B-Tm	Baitoushan	10th century	(3)	—
Ko-g	Hokkaido-Komagatake	6.6–7.2	(4)	plg, opx, cpx, opq
Ng-a	Nigorikawa	14–15	(5)	plg, hbl, opx, cpx, opq, qtz
Us-Ka	Usu	19–18	(6)	plg, hbl, opx, cpx, opq
Ko-i	Hokkaido-Komagatake	37–40	(5)	plg, opx, cpx, opq
Spfl	Shikotsu	46	(6)	plg, opx, cpx, opq
Kt-2	Kuttara	46–50	(7) (8)	plg, opx, cpx, opq
Km-1	Shiribetsu	70–50	(8)	plg, qtz, hbl, cpx, opx (±bt)
Tpfl	Toya	106	(9)	plg, qtz, hbl, opx,cpx, opq

(1) Soya et al. (2007), (2) Katsui et al. (1989), (3) Machida and Arai (2003), (4) Yoshimoto et al. (2008), (5) Ganzawa et al. (2005), (6) Goto et al. (2013), (7) Uesawa et al. (2016), (8) Goto et al. (2020), (9) Matsu'ura et al. (2014).

genesis, mechanism of the sector collapse, duration of dormancy, and evaluation of volcanic hazards. For example, the duration of pre-historical activity depends on the timing of the sector collapse and ranges from <1 to 13 kyr. Thus, the timing of the sector collapse must be confirmed.

Our study investigates the tephrostratigraphy and tephrochronology above and adjacent to the ZDA deposit. In this study, we recognize reworked ash fall deposits on and around the ZDA deposit. We discuss the relationship between the ash deposits and transport and emplacement of the ZDA. In final, we revise the age of collapse and thus the timeframes of pre-historical volcanic activity at Usu volcano.

2 General geology of Usu volcano

2.1 The basement rocks

The basement underlying Usu volcano to the south mainly comprises Plio- and Pleistocene volcanic rocks, the Kaminagawa Formation, and the Toya pyroclastic flow (Tpfl) deposit, from the oldest to youngest (Soya et al., 2007) (Figure 2). The Plio- and Pleistocene volcanic rocks are hydrothermally altered andesites and are distributed in the western to southwestern flank of Usu volcano. The Kaminagawa Formation is an unconsolidated Pleistocene conglomerate, distributed along the Osarugawa River. The Tpfl deposit is found in the eastern to southeastern ring plain of Usu volcano and forms a pyroclastic flow plateau along the Osarugawa River, where it is non-welded and 100 m in thickness. The pyroclastic flow deposits did not accumulate west and southwest of Usu volcano because the mountain formed by Plio- and Pleistocene volcanic rocks created a barrier at the time of the Tpfl eruption.

2.2 Usu volcano

Usu volcano is one of the post-caldera volcanoes of the Toya volcano (Figure 1). The caldera-forming eruption occurred at 106 ka (Matsu'ura et al., 2014) and produced the Tpfl deposit (>37 km^3: Goto et al., 2018), associated with voluminous co-ignimbrite ash (Toya tephra, >150 km^3: Machida et al., 1987). Toya caldera is ca. 12 km in diameter and surrounded by a vast pyroclastic flow plateau. Two post-caldera volcanoes, Nakajima and Usu, formed. Usu volcano formed on the southern rim of the caldera. The volcanic edifice comprises a stratovolcano with a summit crater 2 km in diameter and is associated with the parasitic Donkoroyama cone (Soya et al., 2007). In addition, many lava domes and cryptodomes have formed not only within the summit crater but also at the base of the edifice (Figure 2: Yokoyama et al., 1973; Soya et al., 2007).

The activity of Usu volcano can be divided into pre-historical and historical stages, separated by a long period of dormancy. Pre-historical activity started with the eruption of the Usu-Kaminagawa (Us-Ka) tephra, which comprised an andesitic lower pumice fall deposit and an upper ash fall deposit (Yamagata and Machida, 1996; Goto et al., 2013). After the activity, a stratovolcano was formed by moderate, repeated eruptions of basalt and basaltic andesitic magma, producing lavas (Usu somma lava) and scoria falls. Scoria fall deposits with lapilli ash size (Usu somma tephra) have been recognized at several sites on the flank (Yamagata and Machida, 1996; Miyabuchi et al., 2014). A sector collapse occurred sometime after the establishment of the stratovolcano, resulting in the formation of a scar that opened southwest and the emplacement of the ZDA deposit (Yokoyama et al., 1973; Soya et al., 2007). Juvenile materials related to the collapse event have not yet been identified (Soya et al., 2007; Goto et al., 2019). The timing of the sector collapse was initially thought to be 9–6 ka (Oshima, 1968; Yokoyama et al., 1973)

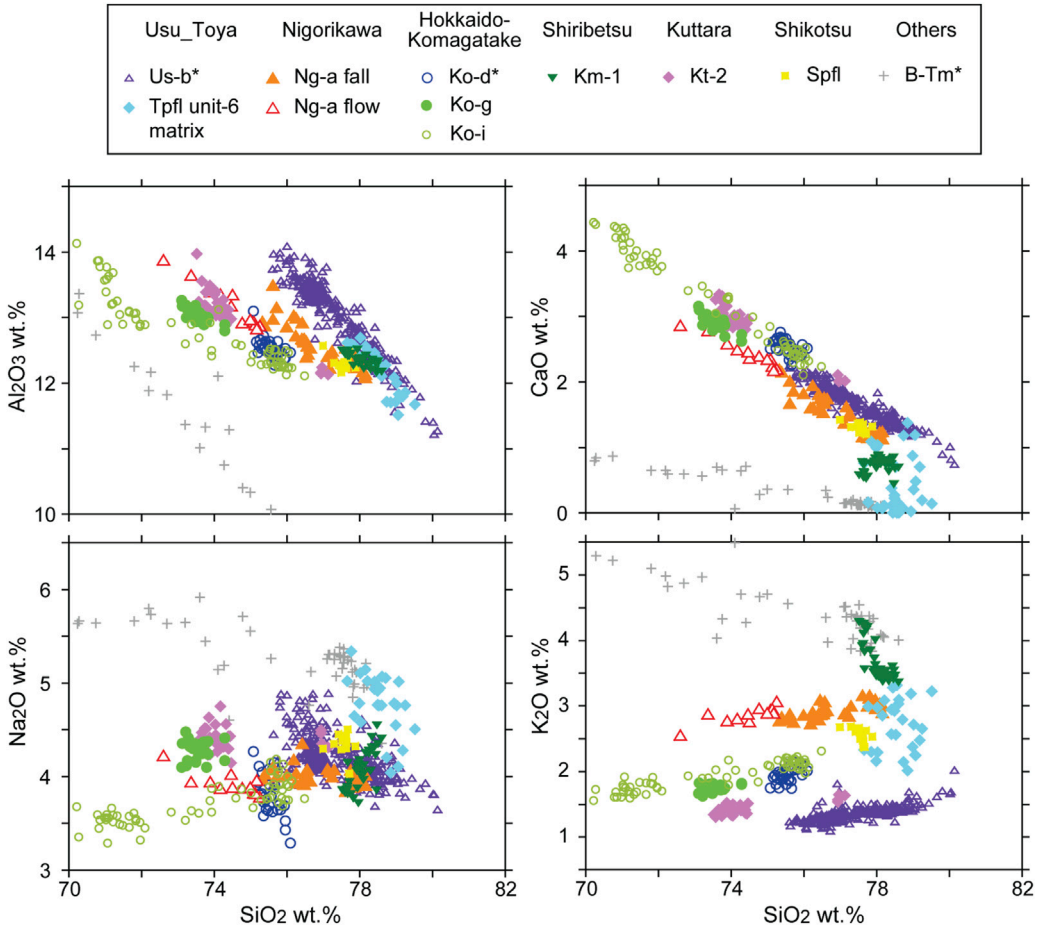

FIGURE 3
Selected SiO_2 variation diagrams for chemical compositions of glass shards from marker tephras recognized around Usu volcano. The distinctive chemical variations of each marker tephra were used to correlate the investigated ash deposits. Asterisks mark tephras whose chemical compositions are determined by the electron probe micro analyzer (EPMA) from Takahashi and Nakagawa (2013), Matsumoto and Nakagawa (2010) and Nakagawa unpublished data.

with more recent estimated ages ranging from >20 to 16 ka (Miyabuchi et al., 2014; Fujine et al., 2016; Goto et al., 2019). After the collapse, the volcano remained dormant for several thousand years or more, until historical activity began. The duration of dormancy has not been clarified because the timing of the collapse remains controversial.

The historical activity of the Usu volcano ended the dormancy in AD 1663, with the most explosive and voluminous Plinian eruption. Since then, eight eruptions have occurred until AD 2000 (Yokoyama et al., 1973; Nakagawa et al., 2005; Soya et al., 2007). Although it has been considered that the AD 1910 eruption was phreatic, other eruptions produced silicic pyroclastic materials, dome lavas, and cryptodomes. The formation ages of all lava domes were recently clarified based on the temporal systematic change of petrological features of erupting tephra deposits and dome lavas from AD 1663–2000 (Matsumoto and Nakagawa, 2019).

3 Methods

The purpose of this study is to clarify the age of the ZDA deposit, which indicates the timing of sector collapse of Usu volcano. Thus, our geological survey focused on the stratigraphic relationship between the ZDA deposit and overlying tephra layers. In addition, the ages of interbedded soils were determined by radiocarbon dating. The lithofacies of the hummocks in the ZDA deposit were also investigated.

Tephrostratigraphy of the area around Usu volcano has been carried out in previous studies (e.g., Yamagata and Machida, 1996; Soya et al., 2007; Goto et al., 2013, 2018, 2019; Miyabuchi

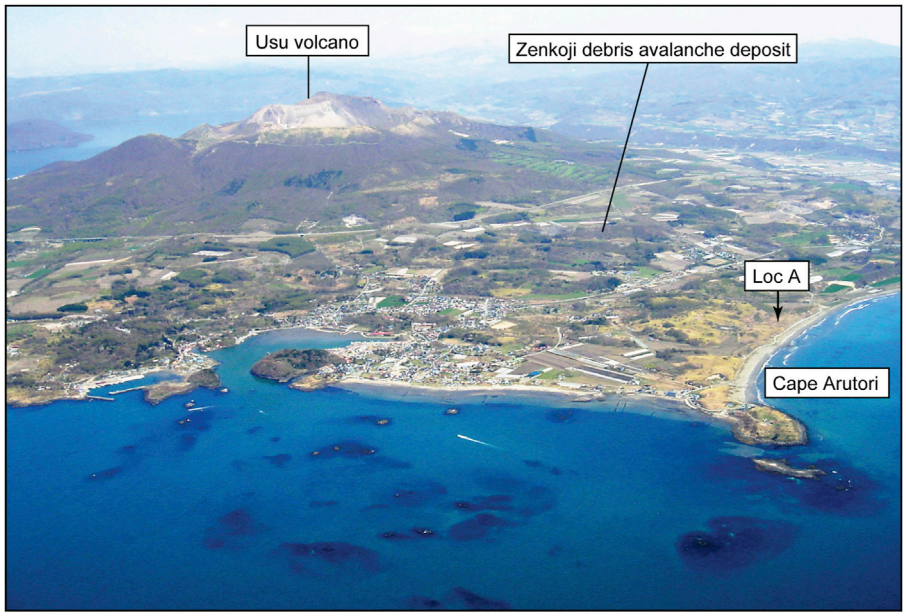

FIGURE 4
Photograph of Usu volcano and the Zenkoji debris avalanche deposit taken from the southwest. Hummocks are also recognized in the sea. Cape Arutori and locality A are indicated (see, Figure 2).

et al., 2014). First, the outcrops described in previous studies were re-investigated. We then concentrated on two localities, A and B (Figure 2). Locality A near Cape Arutori was the same as locality 1 of Goto et al. (2019), who reported the presence of a marker tephra, which directly overlays a hummock. Based on the marker tephra and the presence of charcoal in the hummock, they discussed the timing of the sector collapse of the Usu volcano. On the other hand, locality B is the same as locality 18 in Miyabuchi et al. (2014). They recognized thick reworked tephra layers overlying the scoriaceous tephra layers of the Usu pre-historical stage but did not discuss the reworked tephra. We reinvestigated the tephra sequences of these two outcrops and collected tephra and soil samples.

The characterization and correlation of the tephra layers were carried out using the chemical compositions of the contained glass shards. In addition, the chemical compositions of typical tephra samples collected from the type locality and/or proximal sites were analyzed to correlate each tephra layer. Although Goto et al. (2019) used the refractive index values of glass and minerals, the chemical compositions of these materials were suitable for the correlation of tephra. The chemical composition of the glass shards was determined using an SEM-EDS (scanning electron microscope with energy dispersive spectrometer) system (JEOL JSM-IT200) at Hokkaido University, Japan. For the analysis, 15 kV accelerating voltage and 1.67 nA beam current were used. For prevention of decreased Na, more than 50 μm^2 scanning areas were analyzed for 40 s live time under 15% deadtime. The high reproductivity and accuracy of the analysis could be confirmed using secondary standard samples, such as Lipari obsidian in Italy, and glass shards of Spfa: Shikotsu volcano in Hokkaido, Japan (Supplementary Table S1).

Radiocarbon ages were determined for 13 humic soil samples collected at localities A and B. All samples were analyzed by the Institute of Accelerator Analysis Ltd., Japan, using the accelerator mass spectrometry (AMS) method. Conventional Libby ^{14}C ages (years before present: yBP) were converted into calendar-calibrated ages (calibrated years before present: cal. BP) using the OxCalv4.4 program (Bronk Ramsey, 2009) and IntCal20 radiocarbon age calibration curves (Reimer et al., 2020).

4 Results

4.1 Characteristics of tephra layers around Usu volcano

The age and source volcano of representative tephra layers, younger than Toya tephra (106 ka), recognized in the area around Usu volcano, are listed in Table 1. Except for the B-Tm (Baitoushan-Tomakomai) tephra derived from the Baitoushan volcano at the border between China and North Korea, these tephra layers were derived from

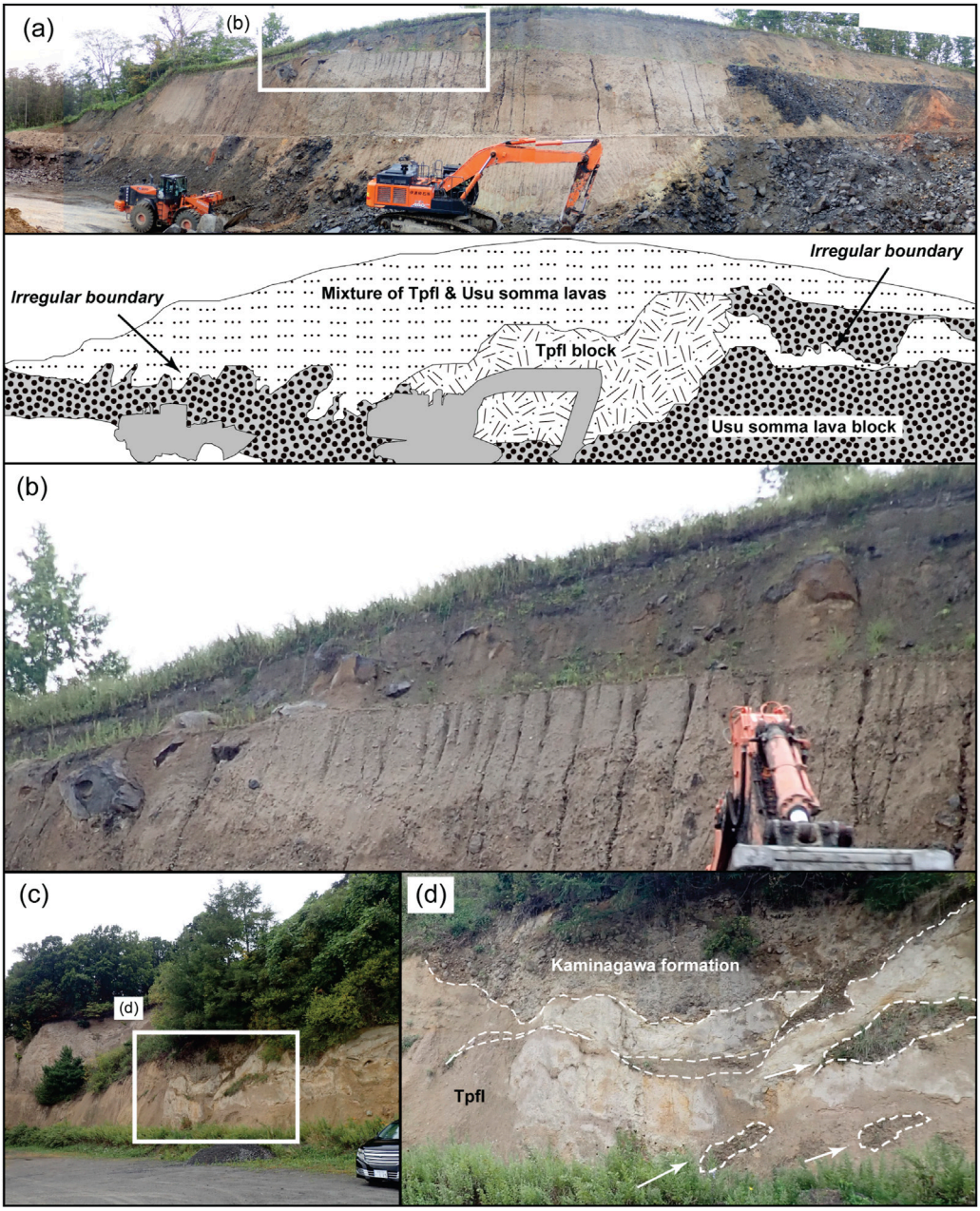

FIGURE 5
Photographs of Zenkoji debris avalanche (ZDA) deposit hummocks. **(A)** Cross-section of a hummock at loc. C. The Usu somma lava block occurs at the base and is overlain by a Toya pyroclastic flow (Tpfl) block. The boundary between both is irregular and often shows flame structures. A mixed facies of Usu somma lava and Tpfl fragments occurs at the top. **(B)** The mixed facies. The Tpfl deposit is dominant in the facies and is fragmented and mixed with disintegrated Usu somma lava clasts. **(C)** Cross-section of a hummock at loc. D. **(D)** The hummock comprises a Tpfl block at the base and the Kaminagawa Formation at the top. The boundary is irregular. The Kaminagawa Formation is deformed and intrudes into the Tpfl block.

volcanoes in southwestern Hokkaido (Figure 1). The major element compositions of the glass shards are shown in selected silica variation diagrams where each tephra forms distinct clusters (Figure 3). SiO_2 contents in almost all analyses were higher than 70%. Several parallel trends formed by individual tephras are recognized in the SiO_2–K_2O diagram. The

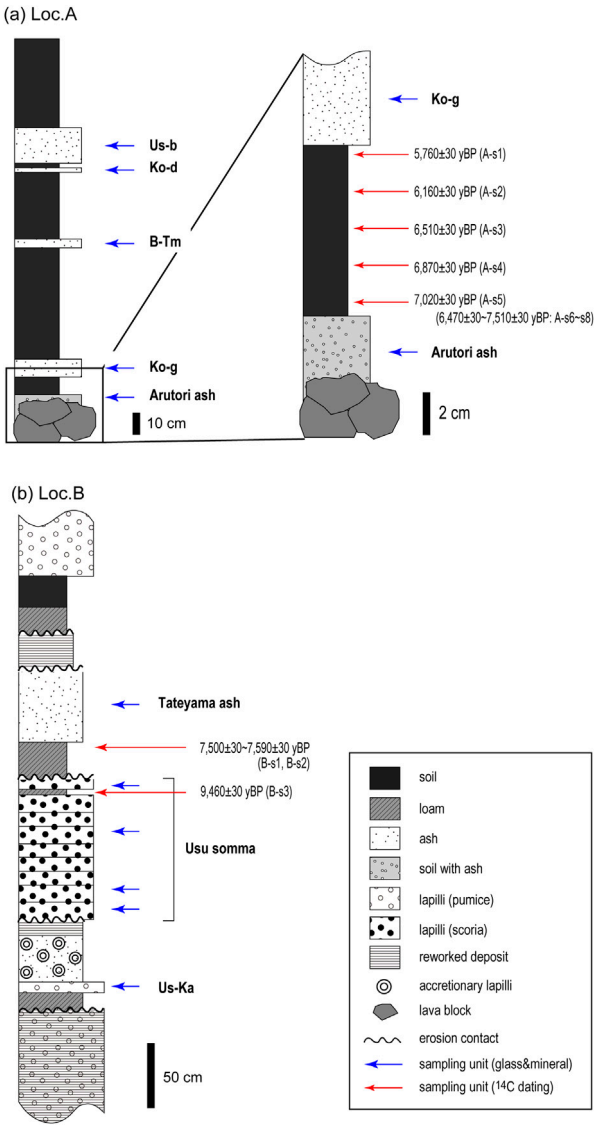

FIGURE 6
Stratigraphic columns of the section at Localities A **(A)** and B **(B)**. Photographs of each section are shown in Figures 7, 10. Stratigraphic positions of tephra and soil samples are marked by a blue and red arrow, respectively. Tephras were correlated to marker tephras (see Table 1) based on chemical compositions of volcanic glass. Radiocarbon ages are also shown. Unknown volcanic ash fall deposits were named Arutori ash at loc. A, and Tateyama ash at loc. B.

geochemical fingerprint of each tephra in Figure 3 later formed the basis for correlating the tephra layers recognized at localities A and B.

4.2 Lithofacies of the Zenkoji debris avalanche deposit

The ZDA deposit is distributed on the southwestern flank of the Usu volcano, extending from the summit to 6–7 km on land (Figure 4). Its width is approximately 5–6 km in NW-SE direction. The volume of the deposit is estimated to exceed 0.3 km^3 (Ui et al., 1986; Goto et al., 2019). The deposit is characterized by many well-preserved hummocky hills (Ui et al., 1986; Yoshida et al., 2012) and consists of 262 hummocks (Yoshida, 2010). These hummocks are composed of three types of lithofacies: basalt and basaltic andesite lavas of the Usu volcano (Usu somma lavas), non-welded silicic pyroclastic flow (Tpfl) deposits, and fluvial deposits of the Kaminagawa Formation (Soya et al., 2007; Miyabuchi et al.,

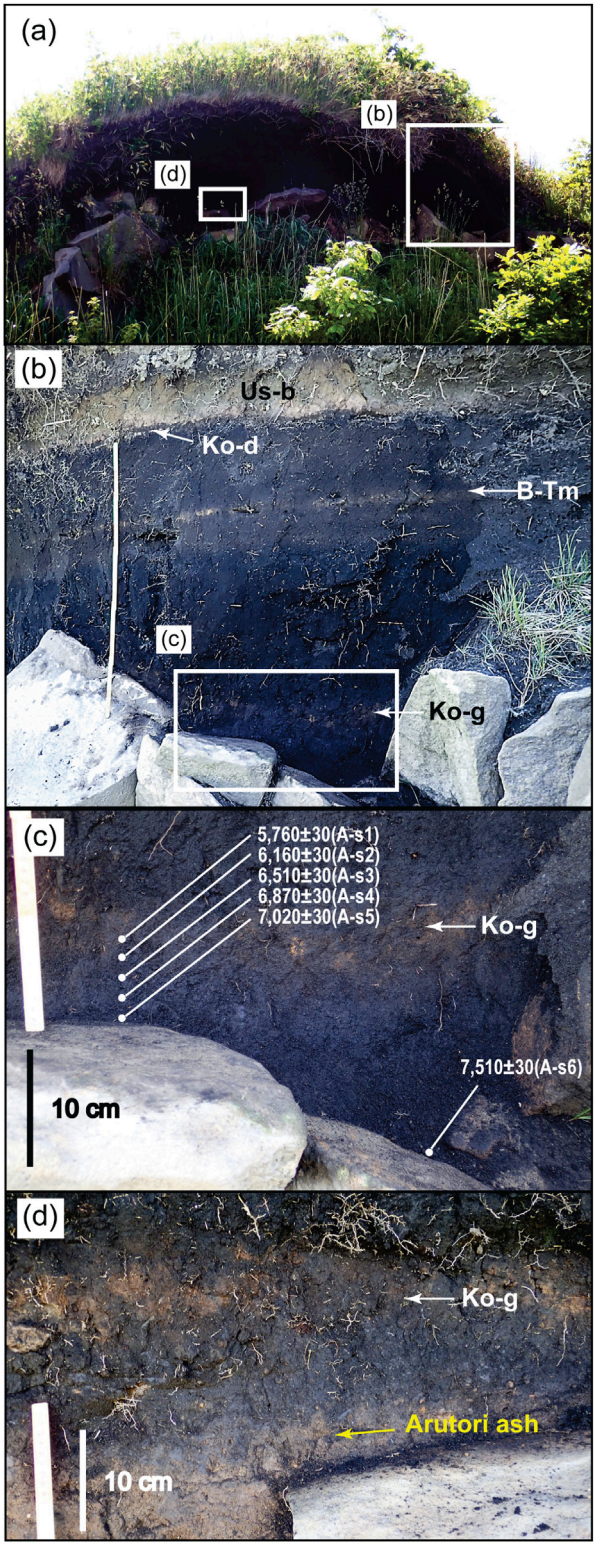

FIGURE 7
(A) Photographs of the cross-section of a hummock at locality A, east of Cape Arutori (Figures 2, 4). **(B)** Close-up of the soil sequence above the ZDA deposit and interbedded four tephra layers, Us-b, Ko-d, B-Tm, and Ko-g, corresponding to the
(*Continued*)

2014; Goto et al., 2019) and were divided into the Usu-somma-type and Toya-dominated-type (Goto et al., 2019). Hummocks near the Usu edifice are mostly of the Usu-somma-type and are mainly composed of Usu somma lavas. On the other hand, Toya-dominated-type hummocks are dominant in the southeastern area and at greater distance from the edifice (Figure 2) and comprise mainly Tpfl deposit accompanied by Kaminagawa Formation. Goto et al. (2019) estimated that the Toya-dominated-type occupies approximately 20 vol. % of total on land hummocks.

Mixture-type hummocks composed of several lithofacies are also common. In these hummocks, the Tpfl deposit is usually deformed and exhibits a complex texture. Goto et al. (2019) pointed out that the hummocks consisting of Usu somma lavas and Tpfl deposit (with the Kaminagawa Formation) preserved the original stratigraphic relationship. Tpfl deposit and Kaminagawa Formation usually occur at the base of the hummock, whereas the Usu somma lavas occur at the top. However, mixture-type hummocks that do not preserve the original stratigraphic relationship are also common. For example, in the locality C hummock (Figure 2), Usu somma lavas occur at the base, overlain by the Tpfl deposit. The boundaries between these blocks are irregular (Figure 5A) and, a mixed facies of the Usu somma lavas and the Tpfl deposit occurs at the top (Figure 5B). Although the Tpfl deposit is dominant in the facies, it was fragmented and mixed with the lavas. In contrast, locality D hummock (Figure 2) comprises the Tpfl deposit at the base and the Kaminagawa Formation at the top separated by an irregular boundary. The Kaminagawa Formation often intrudes into the Tpfl deposit and occurs as a lens (Figures 5C,D). These complex hummock structures were attributed to the non-welded nature of the Tpfl deposit (Goto et al., 2019) and suggest that the Tpfl deposit was mixed with other blocks and fragmented during the transport and emplacement of the ZDA (Dufresne et al., 2021; Paguican et al., 2021).

Inter-hummock deposits were covered by alluvium and are not well exposed. However, if we consider the internal framework of a debris avalanche deposit, it can be assumed that the deposits are composed of matrix facies (Ui et al., 2000; Dufresne et al., 2021) that comprise a mixture of materials

FIGURE 7 (Continued)
stratigraphic section shown in Figure 6A. This section is the same as Figure 8B of Goto et al. (2019). The scale is 1 m. **(C)** Enlarged photograph showing the sampled soil beds and obtained ages. Although Goto et al. (2019) recognized the Ng-a tephra just above the ZDA deposit, we cannot identify the tephra. Note that two soil samples just above the debris avalanche deposit were dated at 7,020 and 7,510 yBP, respectively, which are inconsistent with the age of the Ng-a tephra (15–14 ka). **(D)** Photograph showing obscure ash layer (Arutori ash). See text for details.

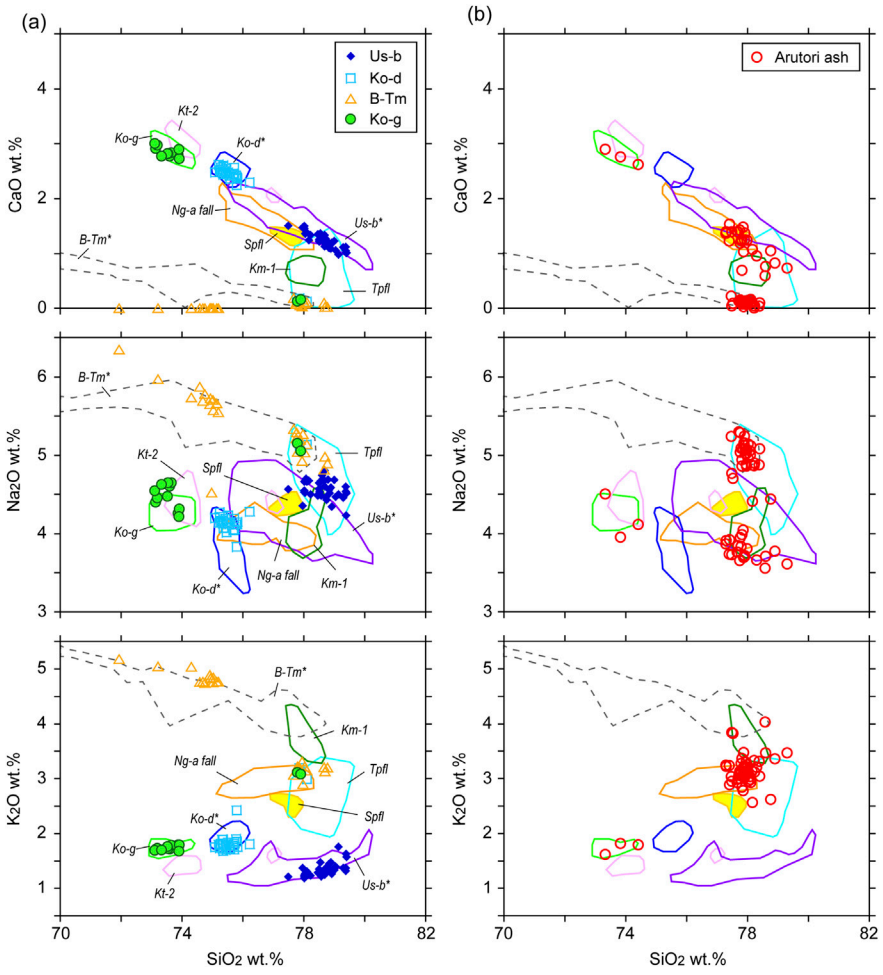

FIGURE 8
Selected SiO_2 variation diagrams for glass shard compositions of tephra layers including the Arutori ash. Compositional fields of each marker tephra derived from Figure 3. **(A)** Four tephra layers, Us-b, Ko-d, B-Tm, and Ko-g form distinct clusters while some glass shards of B-Tm and Ko-g overlap with the field of the Tpfl deposit. Thus, the B-Tm and Ko-g tephras at this outcrop were contaminated with small amounts of Tpfl shards. **(B)** Chemical compositions of glass shards of the Arutori ash form three groups that fall within the fields of the Tpfl ash, Ng-a, and Kt-2 (or Ko-g) with Tpfl shards being the most dominant type. Glass shards plotting in the Ko-g field probably correlate to older tephras of Hokkaido-Komagatake volcano, such as Ko-h.

from the Usu somma lavas, Tpfl deposit, and Kaminagawa Formation.

4.3 Description of outcrops

4.3.1 Locality A: Cape Arutori

Locality A is situated at the southeastern margin of the terrestrial portion of the ZDA deposit (Figure 2). Many hummocks exist in the area and mainly comprise the Toya-dominated-type, but mixture-type composed of the Usu somma lavas and the Tpfl deposit are also recognized. We focused on one of these hummocks (Figure 8 of Goto et al., 2019), which comprises three layers, the Kaminagawa Formation, the Tpfl deposit, and Usu somma lavas, from oldest to youngest. The hummock is overlain by a thick soil which (according to Goto et al., 2019) comprises five marker tephras: Usu 1663 CE (Us-b), Hokkaido-Komagatake 1640 CE (Ko-d), B-Tm, Hokkaido-Komagatake g (Ko-g), and Nigorikawa a (Ng-a) (Goto et al., 2019), from youngest to oldest.

Except for Ng-a tephra, we identify four tephra layers from Us-b to Ko-g tephra in the same outcrop (Figures 6A, 7). Goto et al. (2019) mentioned that Ng-a tephra of 2 cm thickness existed directly on the ZDA deposit. Although we reinvestigate the same section, we do not clearly recognize Ng-a tephra (Figure 7C). On the other hand, at the different positions of the section, we recognize that the soil of 5 cm thick directly on

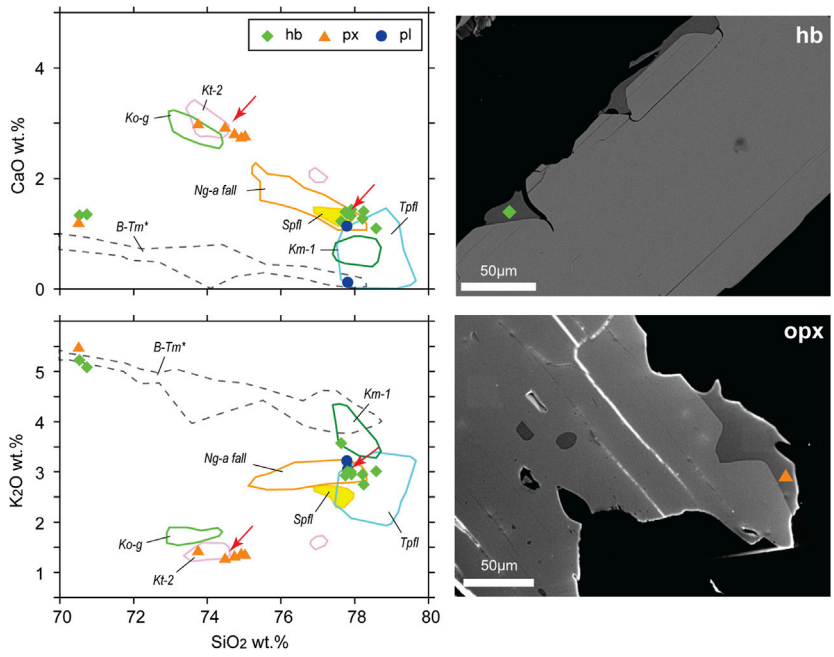

FIGURE 9
Chemical compositions of glass attached to crystals, such as hornblende (hb), orthopyroxene (px), and plagioclase (pl) from the Arutori ash (left). Representative BSE images of crystals with volcanic glass are shown in the right and the glass data of these images are shown by arrows in the left diagrams. Although some glasses plot in the field of the Tpfl deposit and the Ng-a tephra, those associated with orthopyroxene are derived from the Kt-2 tephra (from Kuttara volcano). Glasses with high K_2O contents also exist but the source volcano of these glasses is not known.

the ZDA deposit exhibits a yellowish pale gray color and is rich in volcanic glass compared to normal soil. Although the portion does not exist continuously, it partially mantles the lava block surface and ZDA deposit matrix (Figure 7D), suggesting that the layer is a fall deposit. It contains volcanic glass, free crystals, and lithic fragments. Dominant crystals are plagioclase, hornblende, and orthopyroxene. Moreover, we collected soil samples (A-s1–s6 in Figure 7C) immediately above the ZDA deposit and investigate its components. These also contain a considerable amount of volcanic glass, minerals, and lithic fragments. This suggests that the base portion of the soil is rich in tephra components. Here, we call the portion as "Arutori ash". Considering the stratigraphic position of the ash directly overlying the ZDA deposit, we speculate that the Arutori ash is the same as the Ng-a tephra identified by Goto et al. (2019).

The source volcano and age of each tephra layer can be correlated with a fingerprinted marker tephra based on chemical compositions of the glass shards (Figure 8). While we could confirm three tephra layers, Us-b, Ko-d, and Ko-g, from the outcrop of locality A (Figure 6A), samples from the B-Tm layer contained two types of glass shards, B-Tm and Tpfl. Thus, the B-Tm tephra collected at locality A was contaminated by glass shards from the Tpfl deposit.

Chemical analysis of the glass shards reveals that the Arutori ash were a mixture of several tephras (Figure 8; Supplementary Table S2). Glass shards of the ash correlated with those in the Tpfl deposit were dominant, with Ng-a shards also present as well as glass shards with distinct chemical compositions that can be correlated to either Ko-g or Kt-2 (Kuttara volcano) fields (Figure 8). However, the Ko-g tephra is situated above the Arutori ash. Thus, it could be speculated that glass shards similar to Ko-g tephra might be derived from other older tephras of Hokkaido-Komagatake volcano, such as Ko-h (20 cal. ka) (Yoshimoto et al., 2008). Moreover, the Arutori ash contains several types of minerals. Some of these minerals are partially surrounded by volcanic glass (Figure 9). The chemical compositions of the glasses are shown in Figure 8. While hornblende is present in pumices not only of Ng-a tephra (Yanai et al., 1992) but also of Tpfl deposit (Goto et al., 2018), glasses surrounding the hornblende crystals suggest that these were derived from Ng-a tephra (Figure 9). On the other hand, although orthopyroxene is common in pumice of Tpfl deposit and Ng-a tephra (Yanai et al., 1992; Goto et al., 2018), glass associated with

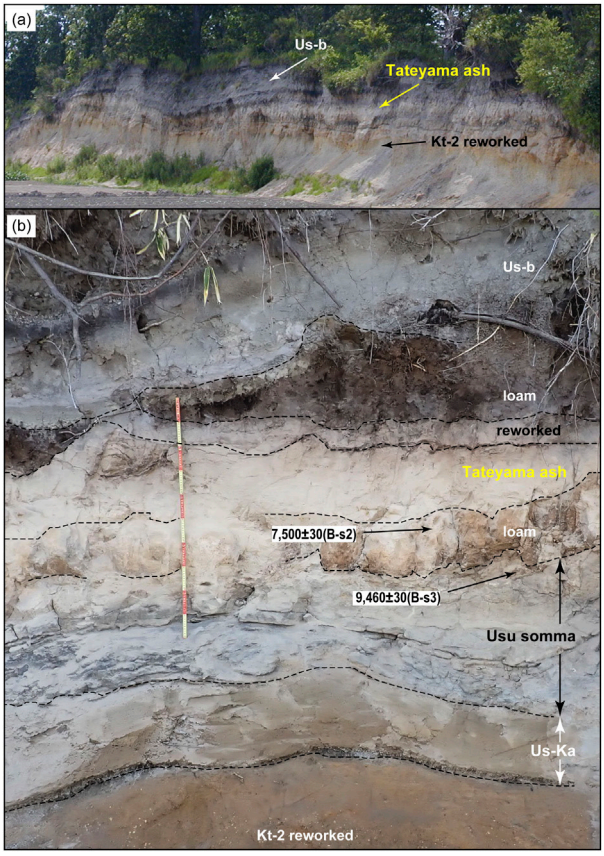

FIGURE 10
(A) Photograph of the outcrop at locality B on the plateau of the Tpfl deposit. The height of the outcrop is 20–10 m. Tephra layers and soil show a mantle bedding structure. **(B)** Close-up photograph of the middle section of the outcrop located 50 m to the right of photograph **(A)**, The stratigraphic section is displayed in Figure 6B.

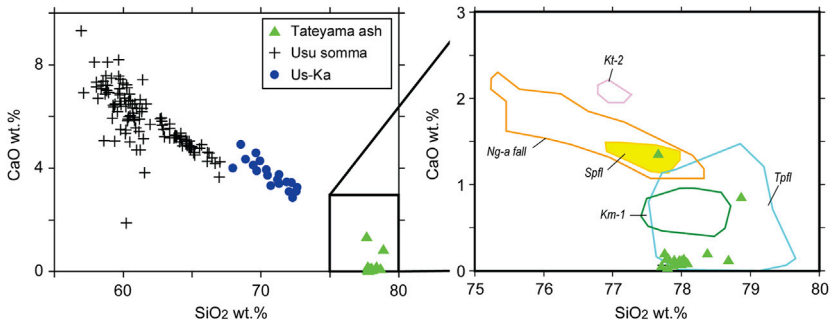

FIGURE 11
SiO_2 vs. CaO diagrams showing the chemical compositions of glass shards from the Us-Ka tephra, the Usu somma tephra, and the Tateyama ash. Most glass shards of the Tateyama ash are correlated to those of the Tpfl deposit.

TABLE 2 Results of the ^{14}C dating of soils collected from Locality A and B around Usu volcano using the accelerator mass spectrometry (AMS) method.

Sample No.	Loc.	Sample type	Method	$\delta^{13}C$(‰) (AMS)	Libby ^{14}C age (yBP)	Calibration range BP (cal. BP, 1σ)	Probability (%)	Calibration range BP (cal. BP, 2σ)	Probability (%)
A-s1	A	Soil	HCl	−26.89 ± 0.41	5,760 ± 30	6,620–6,614	3.7	6,651–6,485	94.7
						6,607–6,585	15.5	6,463–6,457	0.8
						6,565–6,498	49.1		
A-s2	A	Soil	HCl	−28.33 ± 0.44	6,160 ± 30	7,157–7,148	4.8	7,161–6,962	95.4
						7,138–7,106	18.8		
						7,076–6,999	44.7		
A-s3	A	Soil	HCl	−27.47 ± 0.25	6,510 ± 30	7,469–7,448	17.7	7,498–7,415	50.5
						7,433–7,421	19.4	7,398–7,326	45
						7,381–7,355	24.7		
						7,350–7,339	6.5		
A-s4	A	Soil	HCl	−28.32 ± 0.42	6,870 ± 30	7,731–7,666	68.3	7,780–7,655	87.9
								7,646–7,618	7.5
A-s5	A	Soil	HCl	−27.34 ± 0.44	7,020 ± 30	7,927–7,895	27.7	7,936–7,782	95.4
						7,870–7,833	31.7		
						7,810–7,797	8.9		
A-s6	A	Soil	HCl	−24.88 ± 0.22	7,510 ± 30	8,379–8,325	61.4	8,389–8,290	73.9
						8,236–8,224	6.9	8,262–8,206	21.6
A-s7	A	Soil	HCl	−27.47 ± 0.43	6,930 ± 20	7,789–7,701	68.3	7,836–7,682	95.4
A-s8	A	Soil	HCl	−23.89 ± 0.21	6,470 ± 30	7,425–7,419	6.1	7,429–7,321	95.4
						7,387–7,334	62.1		
B-s1	B	Soil	HCl	−24.12 ± 0.36	7,590 ± 30	8,410–8,377	68.3	8,424–8,350	95.4
B-s2	B	Soil	HCl	−22.23 ± 0.21	7,500 ± 30	8,374–8,320	50.9	8,383–8,283	64.9
						8,245–8,218	17.3	8,265–8,200	30.5
B-s3	B	Soil	HCl	−23.31 ± 0.19	9,460 ± 30	10,748–10,655	58.5	11,060–11,045	1.8
						10,619–10,599	9.8	10,998–10,972	4.7
								10,779–10,580	89

orthopyroxene crystals has the same compositions as Kt-2 tephra. Goto et al. (2019) mentioned that the ash just above the ZDA deposit was Ng-a tephra contaminated with Tpfl deposit. However, our analysis of the Arutori ash reveals that the ash is mainly composed of the Tpfl deposit but also contains materials from several younger tephras.

4.3.2 Locality B: Tateyama

Locality B is 2 km east of the ZDA deposit and situated on the Tpfl Plateau along the Osarugawa River (Figure 2). A section 10–20 m in height and 200 m in width exists along a farm (Figure 10A). We identified the tephra sequence as Us-b, Usu somma, Us-Ka, Kt-2, and Tpfl, from top to bottom. The columnar section at locality B is shown in Figure 6B. The Kt-2 tephra is obviously eroded and is overlain by a reworked deposit and loam layer. The Us-Ka tephra above the loam layer can be divided into two subunits: pumice fall and fine ash layers (Figures 6B, 10B), as mentioned by Yamagata and Machida (1996). The 5 cm-thick pumice fall layer comprises well-sorted, poorly vesiculated, light gray pumice (1 cm average diameter). The ash layer overlying the pumice fall is brownish-gray fine ash with weak stratification and several ash beds contain abundant accretionary lapilli (<1 cm diameter). The Us-Ka tephra is overlain by a reworked volcanic ash layer and Usu somma tephra (Figures 6B, 10B). The Usu somma tephra is an alternation of coarse ash fall deposits of basaltic and andesitic scoria. A thin brown soil layer (<1 cm thickness) is observed near the top of the sequence (Figures 6B, 10B). The surface of the Usu somma tephra is obviously eroded and overlain by a reworked deposit (20 cm thick) containing soil layers. The chemical

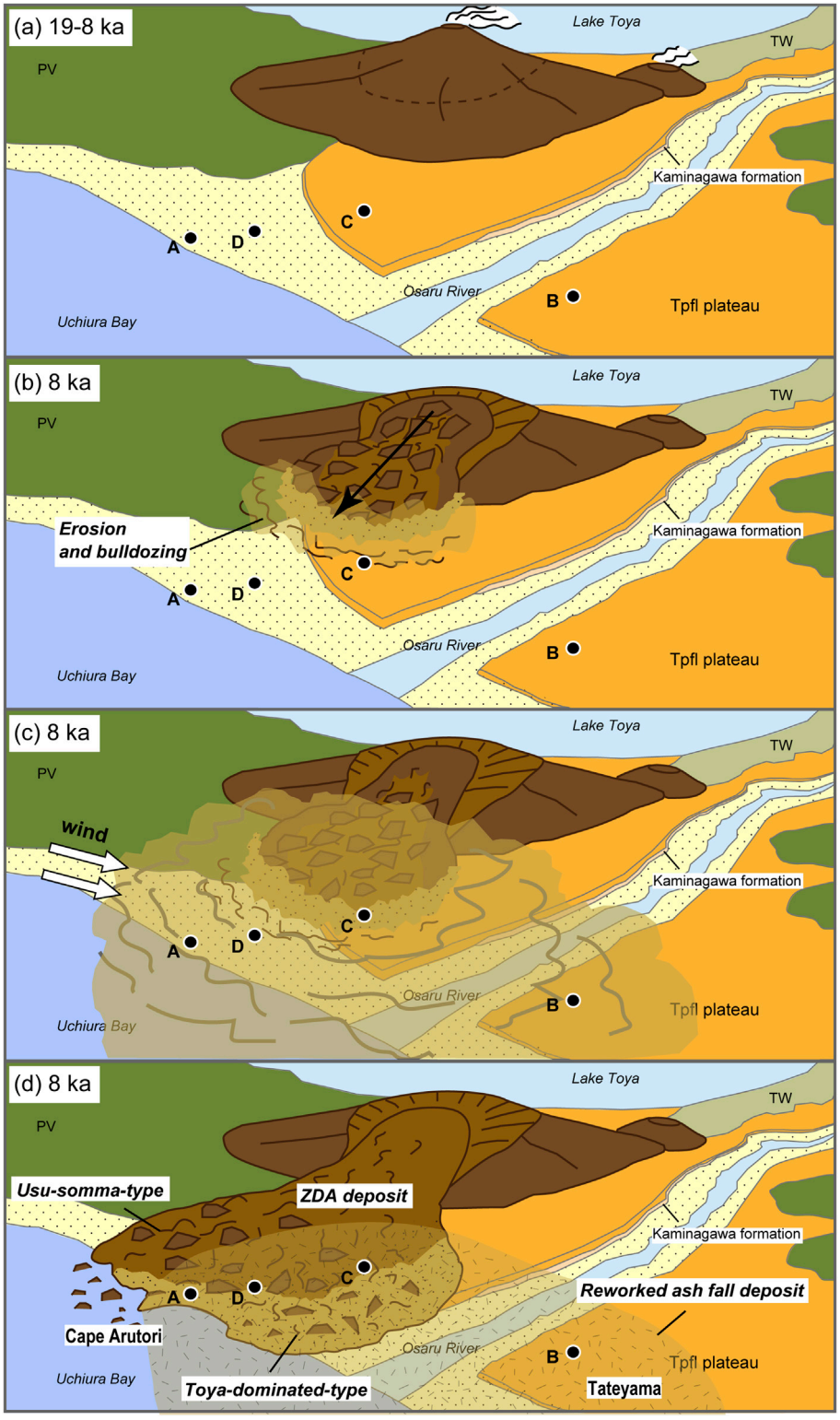

FIGURE 12
Cartoon showing the sequence of the Zenkoji collapse and ZDA generation and emplacement at 8 ka. **(A)** The edifice of Usu volcano was constructed on a basement composed of Plio- and Pleistocene volcanic rocks in the western area, and Tpfl deposit in the eastern area. **(B)** The ZDA was generated by a sector collapse at 8 ka. Dense materials of the collapsed edifice eroded the underlying bedrock along the flow path, especially the Tpfl deposit and the ZDA bulldozed the basement material. The non-welded silicic Tpfl deposit was deformed and fragmented to form an ash cloud of silicic pyroclastic materials. **(C)** Deformation and fragmentation of the Tpfl deposit progressed to form a dense ash cloud, which was dispersed eastward due to prevailing westerly winds. However, the low temperature of the ash cloud prevented it from rising high and ash fall was restricted to proximal areas of the ZDA. **(D)** The ZDA emplaced Toya-dominated-type hummocks (see text) in the southeast area, where the diluted reworked ash settled (the Arutori ash), whereas the denser ash fall occurred east of ZDA deposit (the Tateyama ash).

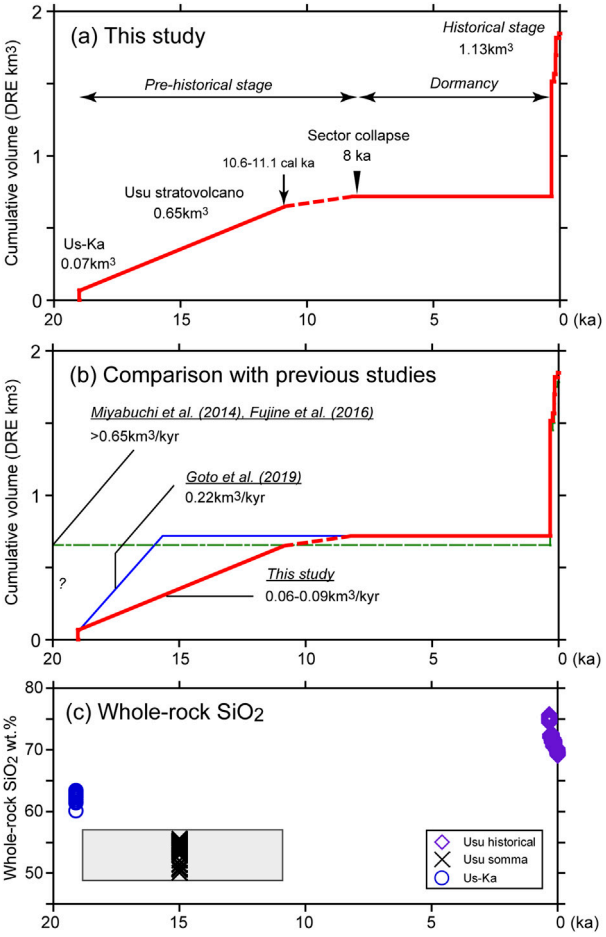

FIGURE 13
(A) The revised magma discharge step-diagram of Usu volcano. Eruption volumes are modified from Oba (1966), Katsui et al. (1981), Takarada et al. (2002) and Goto et al. (2013). **(B)** Comparison of timing of the sector collapse from Miyabuchi et al. (2014), Fujine et al. (2016), Goto et al. (2019) and this study. **(C)** Temporal variation of whole-rock SiO_2 contents of juvenile materials of Usu volcano based on the eruptive history revised by this study. Data of whole-rock chemistry are from Matsumoto and Nakagawa (2010), Kuritani et al. (2016) and Matsumoto (unpublished data).

compositions of volcanic glass of the Us-Ka and Usu somma tephras are shown in Figure 11.

A white fine ash layer (60–20 cm thick) is observed on the soil layer, which we named "Tateyama ash" in this study (Figures 6B, 10B). It is mainly composed of volcanic glass and few free crystals. The ash layer is continuously recognized in the section and exhibited a mantle-bedding structure (Figure 10A), suggesting an air fall origin. Based on the major element chemistry of the glass shards (Figure 11), it can be concluded that the ash is the same as the Tpfl deposit. These indicated that the Tateyama ash was a reworked ash fall deposit. The surface of the ash layer is often eroded and overlain by a reworked layer consisting of several types of fragments, such as brownish-white ash, white ash, and loam. The reworked layer is 30–20 cm thick. The Tateyama ash and overlying reworked deposits are overlain by loam and black soil layers with Us-b and other Usu historical tephras forming the top of the sequence (Figures 6B, 10).

4.4 Radiocarbon ages

At locality A, eight samples were collected from the soil sequence between the Ko-g tephra and ZDA deposit for radiocarbon dating (Table 2). First, to evaluate the accumulation/growth rate of the soil, vertical systematic sampling was carried out at 2 cm intervals (Figures 6A, 7C). The ages of these five samples (A-s1–s5 in Table 2) increased gradually from 5,760 ± 30 yBP for the sample just below the Ko-g tephra to 7,020 ± 30 yBP for the sample just above the ZDA deposit, indicating that the soil was stable and not obviously disturbed. The calibrated age of sample A-s1 immediately below the Ko-g tephra is 6,658–6,457 cal. BP (2σ, ca. 6.6 ka), consistent with the previously reported age of the tephra (6.8 ka: Yoshimoto et al., 2008). Three additional samples above the ZDA deposit were dated (A-s6–s8 in Table 2) and their calibrated ages were 8,389–6,803 cal. BP (2σ).

At locality B, three samples were radiocarbon dated (Table 2). Soil sample B-s3 from the upper part of the Usu somma tephra was dated at 9,460 ± 30 yBP with a calibrated age of 11,060–10,580 cal. BP (2σ). This is the first reported radiocarbon age for the Usu somma tephra. Radiocarbon dates of two samples (B-s1 and s2) of the loam just below the Tateyama ash range from 7,590 ± 30 to 7,500 ± 30 yBP, corresponding to calibrated ages of 8,424–8,200 cal. BP (2σ).

5 Discussion

5.1 Origin and age of the Arutori and Tateyama ash layer

5.1.1 The Arutori ash

Radiocarbon dating of the soil samples at locality A conclude that the Arutori ash was not Ng-a tephra, but a mixture of different tephras. Since the Arutori ash is the obscure tephra layer containing soil components and directly overlays the ZDA deposit, the ages of soil samples A-s5–s8 just above the ZDA deposit indicate the age of the Arutori ash and Ng-a tephra of Goto et al. (2019), for which calibrated ages ranged from 8,389 to 7,321 cal. BP. In the calculation of average age, samples showing maximum and minimum ages were deleted, giving an average age of 7.8 ka. Thus, the age of the Arutori ash is estimated to

be >7.8 ka, which is inconsistent with that of the Ng-a tephra (14–15 ka). A tephra of that age has not been recognized in the area around the Usu volcano (Table 1). In addition, the Arutori ash contains several types of tephra compositions that were correlated to Tpfl (106 ka), Kt-2 (around 50 ka), Hokkaido-Komagatake (unknown age), and Ng-a (14–15 ka) tephras. Thus, we conclude that the Arutori ash (the Ng-a tephra in Goto et al., 2019) is not Ng-a tephra but a reworked ash fall deposit.

This is also consistent with the thickness and accumulation rate of soils between tephras at locality A (Figures 6A, 7B). The thickness of the soil between the Arutori ash (>7.8 ka) and the Ko-g (6.8 ka) is approximately 10 cm, whereas that between the Ko-g and B-Tm (1 ka) is approximately 60 cm, in line with the ages of the layers. If the Arutori ash was the Ng-a tephra (14–15 ka), the thin soil layer between the Ko-g tephra and the Arutori ash would not fit the stratigraphic relationships of the sequence. Thus, the thickness of the interbedded soils between the tephras also supports our findings that the Arutori ash is not the Ng-a tephra.

5.1.2 The Tateyama ash

The Tateyama ash layer is mainly composed of fine glass shards and rarely contains any free crystals. The chemical compositions of these glass shards overlap with those of the Tpfl deposit (Figure 11). No glass shards with chemical compositions distinct from those of the Tpfl deposit were found, indicating that the Tateyama ash is a thick (>20 cm), pure volcanic ash, solely composed of fine particles derived from the Tpfl deposit. The calibrated ages of the two loam samples immediately below the Tateyama ash were 8,424–8,200 cal. BP, giving an estimated depositional age for the Tateyama ash of <ca. 8.3 ka, which is inconsistent with that of the Tpfl deposit (106 ka). In addition, no 8 ka tephra has been identified in this area (Table 1). Thus, we conclude that the Tateyama ash is a reworked ash fall deposit mainly composed of glass shards of the Tpfl deposit with an age of <ca. 8.3 ka.

5.2 Reworked volcanic ash fall caused by a debris avalanche

We recognized two reworked ash fall deposits, Arutori and Tateyama ash, above and east of the ZDA deposit, respectively. The estimated depositional ages of these ashes are nearly the same, ca. 8 ka, and both ash deposits are mainly composed of Tpfl glass shards. This suggests that the event causing the reworking of the Tpfl deposit occurred at ca. 8 ka. The non-welded Tpfl deposit is widely distributed around Usu volcano. Thus, aeolian ash from the Tpfl deposit is always present in this area, particularly during the dry season and is often detected in younger soil and tephra layers. However, in the case of the Arutori and Tateyama ash, a considerable amount of reworked Tpfl ash accumulated, indicating that a dense ash cloud formed during a specific event.

The Arutori ash directly overlays the ZDA deposit, suggesting that the formation of this ash cloud is related to the generation and emplacement of the ZDA. It is well-known that debris avalanches erode and incorporate material from underlying deposits during transportation (e.g., Ui et al., 2000; Yoshida and Sugai, 2007; Zernack et al., 2009: Roverato et al., 2015; Dufresne et al., 2021). Another process for the incorporation of materials from the basement is gravitational spreading of the flank (e.g., van Wyk de Vries and Farncis, 1997; van Wyk de Vries et al., 2001; Paguican et al., 2012) and bulldozing of the underlying strata (Belousov et al., 1999, 2018). Field observations of the internal structures of ZDA hummocks suggest that the Tpfl deposit and Kaminagawa Formation were ripped-up and deformed during the flow of the ZDA (Figure 5D). A mixture of fragments of Usu somma lavas and Tpfl deposit was often recognized in the hummock (Figure 5A), suggesting that fragmentation of the Tpfl deposit progressed during the ZDA flow (e.g., Alloway et al., 2005; Zernack et al., 2009; Dufresne et al., 2021). These fragmentation and elutriation processes produced ash clouds consisting of fine-grained Tpfl material.

The mechanism for the formation of reworked ash by the collapse-generated debris avalanche at Usu volcano is shown in Figure 12. When the sector collapse of Usu volcano occurred (Figure 12A), owing to gravitational spreading and erosion of underlying bedrock, the Tpfl deposit and the Kaminagawa Formation that underly the southeastern flank of the volcano was bulldozed and incorporated by the ZDA. Subsequently, the deformation and fragmentation of the soft Tpfl deposit progressed during debris avalanche flow, resulting in the formation of an ash cloud. On the other hand, the dense Plio- and Pleistocene volcanic rocks underlying the western flank of the volcano were not significantly eroded by the ZDA (Figure 12B). The ash cloud did not rise significantly because the temperature was low. Thus, the reworked ash cloud was deposited locally on top and near the ZDA deposit in downwind areas. Thick reworked ash fall deposits, such as the Tateyama ash, are only recognized east of the ZDA deposit, suggesting a predominantly westerly wind at the time. In contrast, ash comprising glass shards and slightly heavier particles (minerals and lithics) formed a thin fall unit directly above the ZDA deposit (Arutori ash) (Figure 12C). The Toya-dominated hummocks represent bulldozed substrata that settled at the southeastern front of the ZDA deposit, whereas the Usu-somma-type hummocks were distributed along the western front and near the flank of the volcano (Figure 12D).

5.3 Timing of the Zenkoji sector collapse at Usu volcano

In this study, we revealed the presence of reworked volcanic ash fall deposits at two localities and interpreted that the reworked ash was produced by the flow of ZDA. Thus, the ages of these deposits could directly indicate the timing of sector collapse. In the previous section, the ages of the soil samples just above the reworked ash (the Arutori ash) and the hummock of the ZDA were estimated to be >7.8 ka. In contrast, the age of the soil samples just below the reworked ash layer (the Tateyama ash) was estimated to be <8.3 ka. Thus, it can be concluded that sector collapse occurred at ca. 8 ka.

Until this study the age of the sector collapse of Usu volcano has been highly debated and controversial. Oshima (1968) estimated that the timing was 9–6 ka, based on archaeological remnants (Jomon cultural age) and the relationship between the subaqueous distribution of the ZDA deposit and the paleo-sea level. The age estimated by Oshima (1968) was accepted by Yokoyama et al. (1973) and Soya et al. (2007) and modified to 8–7 ka. Our estimated age is similar to that proposed by Oshima (1968), suggesting that the estimation using both remnants and the paleo-sea level might be correct.

On the other hand, previous studies have determined the ages of soil, wood, and charcoal samples in the ZDA, and concluded that these ages (>20 ka–16 ka) could indicate the timing of sector collapse (Kobayashi et al., 2006; Miyabuchi et al., 2014; Fujine et al., 2016; Goto et al., 2019). However, these ages are much older than our conclusion. This suggests that the radiocarbon age dating for materials in the ZDA deposit do not directly indicate the timing of the sector collapse of the Usu volcano but instead represent maximum ages (Ui, 2017; Okuno et al., 2020).

5.4 Revised eruptive history of Usu volcano and its implications

The revised magma discharge step-diagram of Usu volcano, which shows the features of the long-term eruptive activity of the volcano, is shown in Figure 13A. The volcano started its activity at 19–18 ka (Goto et al., 2013) and its eruptive history can be divided into two stages, pre-historical and historical, separated by sector collapse followed by a long period of dormancy (Soya et al., 2007). In this study, we revealed not only the timing of the collapse, but also the timeframes of the pre-historical activity. The age (11 ka) of the soil overlying the Usu somma tephra that represent the pre-historical activity suggests that the stratovolcano had been gradually formed since 19–18 ka until at least 11 ka.

Based on the previously reported timings of the sector collapse, Miyabuchi et al. (2014) and Goto et al. (2019) suggested that the Usu stratovolcano was constructed over a short period and that the sector collapse occurred immediately after the formation of the stratovolcano (Figure 13B); however, our study shows that the growth period of the stratovolcano was much longer. Moreover, Goto et al. (2019) discussed that the overloading of the volcanic edifice on the soft basement due its rapid growth (over ca. 3 kyr) caused the sector collapse. However, we revealed that the stratovolcano had not been constructed this rapidly, but that eruptive activity continued for at least 8 kyr. This finding is inconsistent with that of Goto et al. (2019); thus, the trigger mechanism and processes of the Zenkoji sector collapse should be re-investigated.

Magma compositions of Usu volcano changed significantly from mafic to silicic after the dormancy (Figure 13C). It is essential to know the precise duration of the dormancy to discuss magmatic processes changing magma compositions. However, the duration of the dormant period of Usu volcano was also controversial and according to previous studies (Oshima, 1968; Fujine et al., 2016; Goto et al., 2019) it ranged from 19 to 5.5 kyr. Thus, the temporal change in the magma system beneath Usu volcano should be discussed using the duration of the dormant period (7.5 kyr), which was confirmed in this study.

6 Conclusion

For the first time, we recognized reworked ash fall deposits that were directly produced by the transport and emplacement of a debris avalanche caused by sector collapse of Usu volcano, Japan. Radiocarbon ages of the soil samples just above and below the deposits confirmed the timing of the collapse to be ca. 8 ka. The reworked ash material within these units was derived mainly from silicic, non-welded pyroclastic flow deposits (Toya pyroclastic flow deposits) that are distributed around the volcano. These soft volcanic deposits were ripped-up, deformed and fragmented during transport and emplacement of the debris avalanche, resulting in the formation of an ash cloud. The produced ash particles settled on and around the debris avalanche deposits. Previous studies suggested that the edifice grew rapidly and soon collapsed followed by a long dormancy of >15 kyr. In this study, we revealed that the edifice was gradually constructed over 10 kyr and that the dormant period was ca. 7.5 kyr. Although sector collapse is a low frequency phenomenon, it presents a high-magnitude hazard and it is thus important to recognize such events to better understand the history of the volcanic system and future hazards. However, it is often difficult to determine the exact age and trigger mechanism of collapse. Here we demonstrate for the first time that a reworked ash fall deposit generated by a debris avalanche can be a direct indicator of the timing of a sector collapse.

Data availability statement

The raw data supporting the conclusions of this article will be made available by the authors, without undue reservation.

Author contributions

MN was responsible for the idea, field survey, data interpretation, and manuscript writing. AM also contributed to the field survey, data analysis, interpretation, and manuscript writing. MY analyzed the samples.

Funding

This study was supported by the MEXT "Integrated Program for Next Generation Volcano Research and Human Resource Development" and JSPS KAKENHI (Grant Numbers 19H01980 and 15H03745, respectively).

Acknowledgments

We thank H. Nomura and K. Nakamura of Hokkaido University for preparing the thin sections. We also thank T. Hasegawa of Ibaraki University for providing us with Ng-a pumices. This paper was improved by constructive comments of Jorge E. Romero, Anke Zernack, and Karoly Nemeth.

Conflict of interest

The authors declare that the research was conducted in the absence of any commercial or financial relationships that could be construed as a potential conflict of interest.

Publisher's note

All claims expressed in this article are solely those of the authors and do not necessarily represent those of their affiliated organizations, or those of the publisher, the editors and the reviewers. Any product that may be evaluated in this article, or claim that may be made by its manufacturer, is not guaranteed or endorsed by the publisher.

Supplementary material

The Supplementary Material for this article can be found online at: https://www.frontiersin.org/articles/10.3389/feart.2022.967043/full#supplementary-material

References

Alloway, B., McComb, P., Neall, V., Vucetich, C., Gibb, J., Sherburn, S., et al. (2005). Stratigraphy, age, and correlation of voluminous debris-avalanche events from an ancestral Egmont Volcano: implications for coastal plain construction and regional hazard assessment. *J. R. Soc. N. Z.* 35, 229–267. doi:10.1080/03014223.2005.9517782

Belousov, A., Belousova, M., and Voight, B. (1999). Multiple edifice failures, debris avalanches and associated eruptions in the Holocene history of Shiveluch volcano, Kamchatka, Russia. *Bull. Volcanol.* 61, 324–342. doi:10.1007/s004450050300

Belousov, A., Belousova, M., Zaw, K., Streck, M. J., Bindeman, I., Meffre, S., et al. (2018). Holocene eruptions of Mt. Popa, Myanmar: Volcanological evidence of the ongoing subduction of Indian plate along arakan trench. *J. Volcanol. Geotherm. Res.* 360, 126–138. doi:10.1016/j.jvolgeores.2018.06.010

Bernard, B., TakaradaAndrade, S. S. D., and Dufresne, A. (2021). "Terminology and strategy to describe large volcanic landslides and debris avalanches," in *Volcanic debris avalanches*. Editors M. Roverto, A. Dufresne, and J. N. Procter (Cham: Springer), 51–73. Advances in Volcanology. doi:10.1007/978-3-030-57411-6_3

Boudon, G., Villemant, B., Friant, A., Paterne, M., and Cortijo, E. (2013). Role of large flank-collapse events on magma evolution of volcanoes. Insights from the Lesser Antilles Arc. *J. Volcanol. Geotherm. Res.* 263, 224–237. doi:10.1016/j.jvolgeores.2013.03.009

Bronk Ramsey, C. (2009). Bayesian analysis of radiocarbon dates. *Radiocarbon* 51 (1), 337–360. doi:10.1017/s0033822200033865

Cortes, A., Macias, J. L., Capra, L., and Garduno-Monroy, V. H. (2010). Sector collapse of the SW flank of Volcan de Colima, Mexico. The 3600 yr BP La Lumbre-Los Ganchos debris avalanche and associated debris flows. *J. Volcanol. Geotherm. Res.* 197, 52–66. doi:10.1016/j.jvolgeores.2009.11.013

Costa, A. C. G., Marques, F. O., Hildenbrand, A., Sibrant, A. L. R., and Catita, C. M. S. (2014). Large-scale catastrophic flank collapses in a steep volcanic ridge: The Pico-Faial Ridge, Azores triple junction. *J. Volcanol. Geotherm. Res.* 272, 111–125. doi:10.1016/j.jvolgeores.2014.01.002

Dufresne, A., Zernack, A., Bernard, K., Thouret, J. C., and Roverato, M. (2021). "Sedimentology of volcanic debris avalanche deposits," in *Volcanic debris avalanches*. Editors M. Roverto, A. Dufresne, and J. N. Procter (Cham: Springer), p175–210. Advances in Volcanology. doi:10.1007/978-3-030-57411-6_8

Fujine, H., Endo, K., Suzuki, M., Yoshimoto, M., Suzuki, S., Nakamura, K., et al. (2016). Reexamination of the chronological position of Zenkoji debris avalanche of Usu volcano in south Hokkaido, Japan: in relation to paleoenvironmental changes during the past 20 ka on the Usu coast. *Daiyonki-kenkyu.* 55, 253–270. (in Japanese with English abstract). doi:10.4116/jaqua.55.253

Ganzawa, Y., Koto, N., Yanai, S., and Sadakata, N. (2005). Discovery of primary tephra layers and research of the early stage of the volcanic history of Hokkaido-Komagatake volcano, Japan. *Jour. Geol. Soc. Jpn.* 111, 581–589. (in Japanese with English abstract). doi:10.5575/geosoc.111.581

Gaylord, D. R., and Neall, V. E. (2012). Subedifice collapse of an andesitic stratovolcano: The maitahi formation, taranaki peninsula, New Zealand. *Geol. Soc. Am. Bull.* 124, 181–199. doi:10.1130/B30141.1

Goto, Y., Sekiguchi, Y., Takahashi, S., Ito, H., and Danhara, T. (2013). The 18-19 ka andesitic explosive eruption at Usu volcano, Hokkaido, Japan. *Bull. Volcanol. Soc. Jpn.* 58, 529–541. doi:10.18940/kazan.58.4_529

Goto, Y., Suzuki, K., Shinya, T., Yamauchi, A., Miyoshi, M., Danhara, T., et al. (2018). Stratigraphy and lithofacies of the Toya ignimbrite in southwestern Hokkaido, Japan: Insights into the caldera-forming eruption at Toya caldera. *J. Geogr. Zasshi.* 127, 191–227. doi:10.5026/jgeography.127.191

Goto, Y., Danhara, T., and Tomiya, A. (2019). Catastrophic sector collapse at Usu volcano, Hokkaido, Japan: failure of a young edifice built on soft substratum. *Bull. Volcanol.* 81, 37. doi:10.1007/s00445-019-1293-x

Goto, Y., Miyoshi, M., Danhara, T., and Tomiya, A. (2020). Evolution of the quaternary silicic volcanic complex of shiribetsu, Hokkaido, Japan: an example of

ignimbrite shield volcanoes in an island arc setting. *Int. J. Earth Sci.* 109, 2619–2642. doi:10.1007/s00531-020-01906-9

Katsui, Y., Yokoyama, I., and Murozumi, M. (1981). "Usu volcano," in *Field excursion guide to Usu and tarumai volcanoes and noboribetsu spa*. Editor Y. Katsui (Tokyo: The Volcanological Society Of Japan), 1–37.

Katsui, Y., Suzuki, T., Soya, T., and Yoshihisa, Y. (1989). *Geological map of Hokkaido-Komagatake, scale 1:50,000*. Tsukuba: Geological Survey of Japan. (in Japanese with English abstract).

Kobayashi, N., Nyu, E., Ito, S., Yamagata, H., Lomtatidze, Z., Jorjoliani, I., et al. (2006). "Radiocarbon dating of the Usu-6 site," in *Excavation report of Usu-6 site*. Editor Y. Kosugi (Date City, Hokkaido, 145–155. (in Japanese).

Kuritani, T., Tanaka, M., Yokoyama, T., Nakagawa, M., and Matsumoto, A. (2016). Intensive hydration of the wedge mantle at the Kuril arc–NE Japan arc junction: Implications from mafic lavas from Usu volcano, northern Japan. *J. Petrol.* 57, 1223–1240. doi:10.1093/petrology/egw038

Machida, H., and Arai, F. (2003). *Atlas of tephra in and around Japan*. Tokyo: Univ. Tokyo Press. (in Japanese).

Machida, H., Arai, F., Miyauchi, T., and Okumura, K. (1987). Toya ash- a widespread late Quaternary time-marker in northern Japan. *Daiyonki-kenkyu.* 25, 129–145. (in Japanese with English abstract). doi:10.4116/jaqua.26.2_129

Manconi, A., Longpre, M-A., Walter, T., Troll, V., and Hansteen, T. (2009). The effects of flank collapses on volcano plumbing systems. *Geology* 37, 1099–1102. doi:10.1130/G30104A.1

Marques, F. O., Hildenbrand, A., Victoria, S. S., Cunha, C., and Dias, P. (2019). Caldera or flank collapse in the fogo volcano? What age? Consequences for risk assessment in volcanic islands. *J. Volcanol. Geotherm. Res.* 388, 106686. doi:10.1016/j.jvolgeores.2019.106686

Matsu'ura, T., Furusawa, A., Shimogama, K., Goto, N., and Komatsubara, J. (2014). Late Quaternary tephrostratigraphy and cryptotephrostratigraphy of deep-sea sequences (Chikyu C9001C cores) as tools for marine terrace chronology in NE Japan. *Quat. Geochronol.* 23, 63–79. doi:10.1016/j.quageo.2014.06.001

Matsumoto, A., and Nakagawa, M. (2010). formation and evolution of silicic magma plumbing system: petrology of the volcanic rocks of Usu volcano, Hokkaido, Japan. *J. Volcanol. Geotherm. Res.* 196, 185–207. doi:10.1016/j.jvolgeores.2010.07.014

Matsumoto, A., and Nakagawa, M. (2019). Reconstruction of the eruptive history of Usu volcano, Hokkaido, Japan, inferred from petrological correlation between tephras and dome lavas. *Isl. Arc.* 28, e12301. doi:10.1111/iar.12301

Miyabuchi, Y., Okuno, M., Torii, M., Yoshimoto, M., and Kobayashi, T. (2014). Tephrostratigraphy and eruptive history of post-caldera stage of Toya volcano, Hokkaido, northern Japan. *J. Volcanol. Geotherm. Res.* 281, 34–52. doi:10.1016/j.jvolgeores.2014.05.019

Nakagawa, M., Matsumoto, A., Tajika, J., Hirose, W., and Ohtsu, T. (2005). Re-investigation of eruption history of Usu volcano, Hokkaido, Japan: finding of pre-meiwa eruption (late 17th century) between kanbun (1663) and meiwa (1769) eruptions. *Bull. Volcanol. Soc. Jpn.* 50, 39–52. (in Japanese with English abstract). doi:10.18940/kazan.50.2_39

Oba, Y. (1966). Geology and petrology of Usu volcano, Hokkaido, Japan. *Jour. Fac. Sci. Hokkaido Uni. Ser.* 4 (13), 185–236.

Okuno, M., Ui, T., and Kagaya, N. (2020). Radiocarbon dating for refining the age of the Zenkoji debris avalanche deposit, Usu Volcano, Hokkaido, Japan. *Fukuoka Univ. Sci. Rep.* 50, 108–113. (in Japanese with English abstract).

Oshima, K. (1968). The post-glacial history of Usu bay, Hokkaido. *Jour. Geol. Soc. Jpn.* 74, 1–8. (in Japanese with English abstract). doi:10.5575/geosoc.74.1

Ownby, S., Granados, H. D., Lange, R. A., and Hall, C. M. (2007). Volcan Tancitaro, Michoacan, Mexico, 40Ar/39Ar constraints on its history of sector collapse. *J. Volcanol. Geotherm. Res.* 161, 1–14. doi:10.1016/j.jvolgeores.2006.10.009

Paguican, E. M. R., Van Wyk de Vries, B., and Lagmay, A. M. F. (2012). Volcano-tectonic controls and emplacement kinematics of the Iriga debris avalanches (Philippines). *Bull. Volcanol.* 74, 2067–2081. doi:10.1007/s00445-012-0652-7

Paguican, E. M. R., Roverato, M., and Yoshida, H. (2021). "Volcanic debris avalanche transport and emplacement mechanisms Volcanic Debris Avalanches," in *Advances in Volcanology*. Editors M. Roverto, A. Dufresne, and J. N. Procter (Cham: Springer), 143–174. doi:10.1007/978-3-030-57411-6_7

Reimer, P., Austin, W., Bard, E., Bayliss, A., Blackwell, P., Bronk Ramsey, C., et al. (2020). The IntCal20 northern hemisphere radiocarbon age calibration curve (0–55 cal kBP). *Radiocarbon* 62 (4), 725–757. doi:10.1017/RDC.2020.41

Roverato, M., Cronin, S., Procter, J., and Capra, L. (2015). Textural features as indicators of debris avalanche transport and emplacement, Taranaki volcano. *Geol. Soc. Am. Bull.* 127, 3–18. doi:10.1130/B30946.1

Siebert, L. (1984). Large volcanic debris avalanches: characteristics of source areas, deposits, and associated eruptions. *J. Volcanol. Geotherm. Res.* 22, 163–197. doi:10.1016/0377-0273(84)90002-7

Soya, T., Katsui, Y., Niida, K., Sakai, K., and Tomiya, A. (2007). *Geological map of Usu volcano*. 2nd ed. Tsukuba: Geological Survey of Japan. (in Japanese with English abstract).

Takahashi, R., and Nakagawa, M. (2013). formation of a compositionally reverse zoned magma chamber: Petrology of the ad 1640 and 1694 eruptions of Hokkaido-Komagatake volcano, Japan. *Jour. Petrol.* 54, 815–838. doi:10.1093/petrology/egs087

Takarada, S., Hoshizumi, H., Miyagi, I., Nishimura, Y., Miyabuchi, Y., Miura, D., et al. (2002). Proximal deposits of the Usu 2000 eruption. *Bull. Volcanol. Soc. Jpn.* 47, 645–661. (in Japanese with English abstract). doi:10.18940/kazan.47.5_645

Uesawa, S., Nakagawa, M., and Umetsu, A. (2016). Explosive eruptive activity and temporal magmatic changes at Yotei volcano during the last 50, 000 years, southwest Hokkaido, Japan. *J. Volcanol. Geotherm. Res.* 325, 27–44. doi:10.1016/j.jvolgeores.2016.06.008

Ui, T., Yamamoto, H., and Suzuki-Kamata, K. (1986). Characterization of debris avalanche deposits in Japan. *J. Volcanol. Geotherm. Res.* 29, 231–243. doi:10.1016/0377-0273(86)90046-6

Ui, T., Takarada, S., and Yoshimoto, M. (2000). "Debris avalanches," in *Encyclopedia of volcanoes*. Editor H. Sigurdsson (San Diego: Academic Press), 617–626.

Ui, T. (2017). Discussion "chronological position of Zenkoji debris avalanche (Fujine et al. 2016)". *Daiyonki-kenkyu.* 56, 243–244. (in Japanese). doi:10.4116/jaqua.56.243

van Wyk de Vries, B., and Francis, P. W. (1997). Catastrophic collapse at stratovolcanoes induced by gradual volcano spreading. *Nature* 387, 387–390. doi:10.1038/387387a0

van Wyk de Vries, B., Self, S., Francis, P. W., and Keszthelyi, L. (2001). A gravitational spreading origin for the Socompa debris avalanche. *J. Volcanol. Geotherm. Res.* 105, 225–247. doi:10.1016/S0377-0273(00)00252-3

Watt, S. (2019). The evolution of volcanic systems following sector collapse. *J. Volcanol. Geotherm. Res.* 384, 280–303. doi:10.1016/j.jvolgeores.2019.05.012

Yamagata, K., and Machida, H. (1996). "Toya tephra and other overlying tephras at Date-city, Hokkaido,". Committee for Inventory of Quaternary Outcrops in *Inventory of quaternary outcrops –tephras in Japan* (Tokyo: Japan Association for Quaternary Research), 50. (in Japanese).

Yanai, S., Ganzawa, Y., and Komori, Y. (1992). The stratigraphy and distribution of the Nigorikawa tephra, latest glacial age time-marker in southwest Hokkaido. *Jour. Geol. Soc. Jpn.* 98, 125–136. (in Japanese with English abstract). doi:10.5575/geosoc.98.125

Yokoyama, I., Katsui, Y., Oba, Y., and Ehara, Y. (1973). *Usuzan, its volcanic geology, history of eruption, present state of activity and prevention of disasters*. Sapporo: Committee for the Prevention of Disasters of Hokkaido. (in Japanese).

Yoshida, H., and Sugai, T. (2007). Magnitude of the sediment transport event due to the Late Pleistocene sector collapse of Asama volcano, central Japan. *Geomorphology* 86, 61–72. doi:10.1016/j-geomorph.2006.08.006

Yoshida, H., Sugai, T., and Ohmori, H. (2012). Size-distance relationships for hummocks on volcanic rockslide-debris avalanche deposits in Japan. *Geomorphology* 136, 76–87. doi:10.1016/j.geomorph.2011.04.044

Yoshida, H. (2010). Size distribution of debris avalanche hummocks in Japan. *J. Geogr.* 119, 892–899. (in Japanese with English abstract). doi:10.5026/jgeography.119.892

Yoshimoto, M., Miyasaka, M., Takahashi, R., Nakagawa, M., and Yoshida, K. (2008). Reevaluation of the pre-1640 AD eruptive history of Hokkaido-Komagatake volcano, northern Japan. *Jour. Geol. Soc. Jpn.* 114, 336–347. (in Japanese with English abstract). doi:10.5575/geosoc.114.336

Zernack, A. V., and Procter, J. N. (2021). "Cyclic growth and destruction of volcanoes," in *Volcanic debris avalanches. Advances in Volcanology*. Editors M. Roverto, A. Dufresne, and J. N. Procter (Cham: Springer), 311–356. doi:10.1007/978-3-030-57411-6_12

Zernack, A. V., Procter, J. N., and Cronin, S. J. (2009). Sedimentary signatures of cyclic growth and destruction of stratovolcanoes: A case study from Mt. Taranaki, New Zealand. *Sediment. Geol.* 220, 288–305. doi:10.1016/j.sedgeo.2009.04.024

Zernack, A. V., Cronin, S. J., Neall, V. E., and Procter, J. N. (2011). A medial to distal volcaniclastic record of an andesite stratovolcano: detailed stratigraphy of the ring-plain succession of south-west taranaki, New Zealand. *Int. J. Earth Sci.* 100, 1937–1966. doi:10.1007/s00531-010-0610-6